



# Combining Gompertzian growth and cell population dynamics

Frank Kozusko<sup>a,\*</sup>, Željko Bajzer<sup>b,\*</sup>

<sup>a</sup> *Department of Mathematics, Hampton University, Hampton, VA 23668, USA*

<sup>b</sup> *Biomathematics Resource, Mayo Clinic, Rochester, MN 55905, USA*

Received 15 July 2002; received in revised form 21 May 2003; accepted 20 June 2003

---

## Abstract

A two-compartment model of cancer cells population dynamics proposed by Gyllenberg and Webb includes transition rates between proliferating and quiescent cells as non-specified functions of the total population,  $N$ . We define the net inter-compartmental transition rate function:  $\Phi(N)$ . We assume that the total cell population follows the Gompertz growth model, as it is most often empirically found and derive  $\Phi(N)$ . The Gyllenberg–Webb transition functions are shown to be characteristically related through  $\Phi(N)$ . Effectively, this leads to a hybrid model for which we find the explicit analytical solutions for proliferating and quiescent cell populations, and the relations among model parameters. Several classes of solutions are examined. Our model predicts that the number of proliferating cells may increase along with the total number of cells, but the proliferating fraction appears to be a continuously decreasing function. The net transition rate of cells is shown to retain direction from the proliferating into the quiescent compartment. The death rate parameter for quiescent cell population is shown to be a factor in determining the proliferation level for a particular Gompertz growth curve.

© 2003 Elsevier Inc. All rights reserved.

*Keywords:* Gompertz growth model; Cell kinetics; Tumor growth; Proliferation; Quiescence

---

## 1. Introduction

The Gompertz model of growth has been widely and successfully used as a simple, yet adequate descriptor of tumor growth curves [1–11]. Possible theoretical bases of this model have been addressed in the literature from various points of view, and it remains to be a topic of investigation [9,12–24]. Most of the authors have attempted to derive the Gompertz model as an

---

\* Corresponding authors. Tel.: +1-757 727 5352 (F. Kozusko); Tel.: +1-507 284 8584 (Ž. Bajzer).

*E-mail addresses:* [frank.kozusko@hamptonu.edu](mailto:frank.kozusko@hamptonu.edu) (F. Kozusko), [bajzer@mayo.edu](mailto:bajzer@mayo.edu) (Ž. Bajzer).

approximation (or a special case) of more general models, which are deemed to be based on accepted biological foundations. A somewhat similar approach is pursued in this paper: the Gompertz model is postulated (based on its empirical justification) and then the more general model is specified to yield the Gompertz model.

We explore the possibility of embedding the Gompertz model in the well-known two-compartment models of cell population dynamics [16,25–27]. More specifically we will consider the two-compartment model of tumor growth proposed by Gyllenberg and Webb [16]. This model is rather general in a sense that it explicitly incorporates all biologically essential phenomena of cell population dynamics, i.e. proliferation, quiescence and cell loss. Furthermore, the rates for transition from quiescent to proliferative cell subpopulation and the transition from proliferative to quiescent subpopulation are not described just by rate constants, but by two different (unspecified) functions of the total cell population, which can possibly describe regulatory mechanisms in tumor growth. Gyllenberg and Webb found very specific and simple functions for these transition rates, which yield the Gompertz model or the logistic model. Expanding on this idea in the present paper, we define a net inter-compartmental transition rate function whose exact form emerges from the assumption that the total cell population is governed by the Gompertz model. This leads to a general relationship between the individual transition rates. Under this assumption we then solve Gyllenberg–Webb model analytically, and obtained expressions for the quiescent and proliferating subpopulations as functions of time. Further, we determine the expression for the growth fraction, and study its properties. We also explore various relations among parameters of the Gompertz and the Gyllenberg–Webb model. It is shown that transition rates do not necessarily have to be non-decreasing or non-increasing functions as Gyllenberg and Webb assumed.

In the present approach, on one hand we can consider the Gompertz model for total cell population as biologically interpretable within the context of two-compartment cell population dynamics. On the other hand we have determined the unknown transition rates of Gyllenberg–Webb model in such a way that it automatically describes the wealth of tumor growth curves being fitted by the Gompertz model. This is by no means trivial, because some complex models with more free parameters than the Gompertz model could not fit some tumor growth data adequately [9]. In fact many of those more complex models were not validated against data, as it is tacitly assumed that they have enough free parameters to fit simple sigmoidal growth curves.

We wish to point out that our approach is not restricted to tumor growth only. The Gompertz model have been almost universally used to describe the growth of organisms, tissues, and populations of single cell organisms. Additionally the biological assumptions and mathematical generality of the Gyllenberg–Webb model are sufficient to warrant its application to growth in general.

In Section 2 we briefly introduce the Gompertz model to set the notation and to point out some characteristic features. Similarly, in Section 3 we introduce the Gyllenberg–Webb model, and then in Section 4 we propose a way to combine these two models. The main analytical results of this hybridization (relations among transition rates and model parameters, analytical expressions for proliferating and quiescent subpopulations) are presented in Section 5. Section 6 is devoted to discussion of obtained analytical results in the context of simulations. In two appendices we present details of two proofs.

## 2. The Gompertz function

The Gompertz function, which can be expressed as

$$N(t) = N_0 \exp\left[\frac{k_+}{k_-}(1 - e^{-k_-t})\right], \quad N(0) = N_0, \tag{1}$$

generates a sigmoidal curve as exemplified in Fig. 1. For tumor growth modeling,  $N(t)$  describes the number of cells in the tumor at time  $t$  (cellularity).  $N_0$  represents the initial cellularity. In natural tumors  $N_0$  can well be just one cell. For computational convenience in the following, we normalize  $N(t)$  with  $N_0$ . For the normalized  $N(t)$ , which we will not denote differently, obviously it follows  $N(0) = 1$ . Parameter  $k_+$  effectively represents growth rate constant, while  $k_-$  describes the retardation of growth. Both parameters have the dimension of inverse time. Normalized  $N(t)$  is the solution of differential equation

$$\dot{N} = k_+N - k_-N \ln N, \quad N(0) = 1, \tag{2}$$

which more explicitly shows the meanings of  $k_+$  and  $k_-$ .

The Gompertz function has been analyzed in various ways (see e.g. [9]). Here we briefly explore some less known relations between  $k_+$  and  $k_-$ , and the characteristic features of the growth curve: the carrying capacity and the inflection point. The carrying capacity  $N(\infty) \equiv N_\infty$  is naturally assumed to be finite and non-zero. Then, from (1) it follows  $k_- > 0$ , and further, assuming growth (not degradation) it follows

$$N_\infty = e^{\frac{k_+}{k_-}} > 1, \tag{3}$$

and consequently  $k_+ > 0$  as expected.

The inflection point signifies the start of tumor growth deceleration when the maximal rate of growth was achieved. Biological growth as, empirically known, always eventually slows down due to external factors and possible internal growth control. To find the inflection point of the

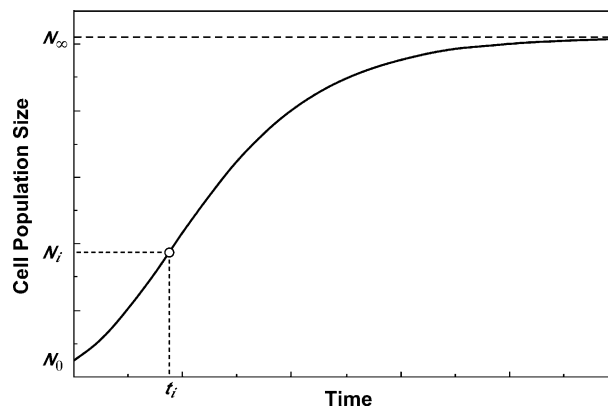


Fig. 1. Typical Gompertz sigmoidal growth curve.  $N_0$  is the initial number of cells,  $N_\infty$  is the maximal number of cells (carrying capacity), and  $N_i$  is the population size at the inflection point achieved at time  $t_i$ .

Gompertz curve,  $N_i$ , it is required that  $\ddot{N} = \{k_+ - k_- \ln N - k_-\} \dot{N} = 0$  and therefore, because  $\dot{N} > 0$  for finite  $t$ ,

$$\ln N_i = \frac{k_+}{k_-} - 1, \quad t_i = \frac{1}{k_-} \ln \frac{k_+}{k_-}, \tag{4}$$

where  $t_i$  is the time when the inflection point is achieved. If  $k_+ < k_-$ , obviously, no inflection point exists, because that would imply decreasing  $N$  and  $N_i < 1$ . From Eqs. (4) and (3) it follows

$$N_i = \exp\left(\frac{k_+}{k_-} - 1\right), \quad N_\infty = eN_i. \tag{5}$$

Thus the tumor can maximally outgrow its size at inflection point by a factor of  $e$ . For times that exceed  $t_i$  (i.e. for times  $t$  such that  $\ddot{N}(t) < 0$ ), it follows  $N(t) > N_i$  and (5) implies the inequality

$$N_\infty < eN(t), \tag{6}$$

which provides an estimate of the upper limit of the carrying capacity if the growth appears to decelerate after reaching the maximal rate. It has to be noted that Gompertz growth curve describes only the trend of growth and does not account for observed stochastic irregularities. Thus the inflection point obtained is just an estimate of the turning point in growth when the observed trend shows decreasing growth rate. Similarly the carrying capacity  $N_\infty$  just estimates the maximal tumor size which in clinical setting may not be achieved.

### 3. Two-compartment population dynamics

A two-compartment model of cell population growth dates back at least 40 years [25]. More recently Gyllenberg and Webb [16] (whose variable/parameter notation will be used here for consistency) have used such a model to show that it yields Gompertz or logistic growth under special parameter selection. The model (Fig. 2) consists of proliferating and quiescent cell compartments; it allows for transition between the compartments and cell death from either compartment. Transition rate functions are considered to be functions of the total number of cells.

The following set of ordinary differential equations describes the model:

$$\dot{P} = [\beta - \mu_p - r_o(N)]P + r_i(N)Q, \tag{7}$$

$$\dot{Q} = r_o(N)P - [r_i(N) + \mu_q]Q, \tag{8}$$

$$N = P + Q, \quad P_0 + Q_0 = 1. \tag{9}$$

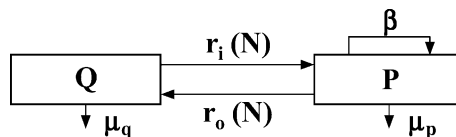


Fig. 2. Two-compartment model of cell population growth which includes proliferating ( $P$ ) and quiescent ( $Q$ ) cell subpopulations. For the meaning of transition rates see text.

$P$  and  $Q$  represent the normalized number of proliferating and non-proliferating (quiescent) cells, and  $\mu_p \geq 0$  and  $\mu_q \geq 0$  represent the death rate parameters for the  $P$  and  $Q$  compartments, respectively.  $\beta > 0$  is the proliferation rate parameter.  $\dot{N} > 0$  for  $t < \infty$  and  $\dot{N}_\infty = 0$  requires  $\beta - \mu_p > 0$ . The transition rate functions are:  $r_o(N) \geq 0$ , describing transition from the proliferation subpopulation into the quiescent subpopulation, and  $r_i(N) \geq 0$  describes the transition into the proliferation subpopulation from the quiescent subpopulation.

#### 4. Combining the Gompertz and the Gyllenberg–Webb model

Our goal is to construct a two-compartment model that specifically predicts Gompertz growth for  $N$ . This idea was briefly introduced in [9], but mistakes were found in the corresponding derivations. Here the idea is extended, and related derivations are revised. We start by defining the net transition rate function:

$$\Phi(N) = r_o(N)P - r_i(N)Q, \tag{10}$$

when  $\Phi(N) > 0$ , the net transition rate is from the proliferating compartment into the quiescent compartment. Using Eqs. (9) and (10), we reform Eqs. (7) and (8) into

$$\dot{P} = [\beta - \mu_p]P - \Phi(N), \tag{11}$$

$$\dot{N} = [\beta - \mu_p + \mu_q]P - \mu_q N. \tag{12}$$

At this point we introduce our crucial assumption, that the growth function for  $N$  is Gompertzian and therefore satisfies (2). It follows

$$\dot{N} = N\delta(N), \quad \ddot{N} = [\delta(N) - k_-]\dot{N}, \quad \delta(N) = k_+ - k_- \ln(N) = \delta = k_+ e^{k_- t}. \tag{13}$$

Taking the time derivative of Eq. (12), using Eq. (11) for  $\dot{P}$ , substituting for  $P$  from Eq. (12) and using Eq. (13) for  $\dot{N}$  and  $\ddot{N}$  yields

$$\Phi(N) = N \left[ \frac{(\beta - \mu_p - \mu_q - \delta(N) + k_-)\delta(N) + \mu_q(\beta - \mu_p)}{\beta - \mu_p + \mu_q} \right]. \tag{14}$$

#### 5. Analysis

Eq. (14) establishes the form of  $\Phi(N)$  that causes the Gyllenberg–Webb model to predict Gompertz tumor growth. In this section we show implications of this relation to the form of rate functions  $r_i(N)$  and  $r_o(t)$ , and subsequently derive relations among parameters of the two models. Furthermore, using prescription (14) we find analytical solution of The Gyllenberg–Webb model (i.e.  $P(t)$  and  $Q(t)$ ) and analyze the behavior of this solution in an analytical manner. Finally, we show that  $\Phi(N) \geq 0$  implying that the Gompertz model of growth requires depletion of the proliferating subpopulation.

The characteristic relationship between  $r_o$  and  $r_i$  can be derived by using Eqs. (12)–(14) and  $Q = N - P$ :

$$(\delta + \mu_q)r_o - (\beta - \mu_p - \delta)r_i = k_- \delta + (\delta + \mu_q)(\beta - \mu_p - \delta). \tag{15}$$

If we express  $r_o$  in terms of  $r_i$  then the requirement

$$r_o = \frac{k_- \delta + (\beta - \mu_p - \delta)(\delta + \mu_q + r_i)}{\delta + \mu_q} \geq 0 \tag{16}$$

implies that one can choose any  $r_i(N) \geq 0$  (not necessarily non-increasing) as long as

$$\delta \leq k_+ \leq \beta - \mu_p. \tag{17}$$

Indeed, assuming  $k_+ > \beta - \mu_p$  one would end up in contradiction because by evaluating Eqs. (12) and (13) at  $t = 0$ , it follows from  $N = 1$  and  $P_0 + Q_0 = 1$  that

$$k_+ = \dot{N}(0) = (\beta - \mu_p)P_0 - \mu_q Q_0. \tag{18}$$

From here assumption  $k_+ > \beta - \mu_p$  yields  $(\beta - \mu_p + \mu_q)Q_0 < 0$  which contradicts requirements  $\mu_p \geq 0, \mu_q \geq 0, \beta - \mu_p \geq 0$  (see Section 3).

Interestingly, if we express  $r_i$  in terms of  $r_o$  and require

$$r_i = \frac{-k_- \delta + (\delta + \mu_q)(\delta + \mu_p - \beta + r_o)}{\beta - \mu_p - \delta} \geq 0, \tag{19}$$

then it follows that  $r_o$  is not completely arbitrary, but for  $k_+ \geq \beta - \mu_p$  should satisfy the inequality

$$r_o \geq \frac{k_- \delta + (\delta + \mu_q)(\beta - \mu_p - \delta)}{\delta + \mu_q}. \tag{20}$$

Stated prescriptions for  $r_i$  and  $r_o$  are certainly more general than the ones originally recommended by Gyllenberg and Webb [16], who assumed that  $r_o(N)$  was non-decreasing and  $r_i(N)$  non-increasing and only derived Gompertz growth for  $r_o(N) = 1 + \log(N)$ .

### 5.1. Expressions for $k_+, k_-$ and $\frac{k_+}{k_-}$

Eq. (18) relates Gompertz growth rate  $k_+$  to rate parameters of Gyllenberg–Webb model. The value of  $k_+$  is equal to the initial growth rate of  $N(t)$  which is set by the difference in the net increase of the proliferating cells and the loss of quiescent cells without the consideration of inter-compartment transition at  $t = 0$ .

Similarly, evaluating  $\dot{N}(0)$  from (13) yields

$$k_- = \dot{N}(0) - \frac{\dot{N}(0)}{N(0)} = \dot{N}(0) - \left( \frac{d\dot{N}}{dN} \right)_{t=0}. \tag{21}$$

Thus,  $k_-$  equals the initial growth rate minus the initial rate of change of the growth rate with respect to the change in  $N$ , which includes the effects of the inter-compartment transitions. Eqs. (21) and (8)–(12) produce a value for  $k_-$  in terms of the parameters of the Gyllenberg–Webb model:

$$k_- = [(\beta - \mu_p)P_0 - \mu_q Q_0] - \left\{ \frac{(\beta - \mu_p)^2 P_0 + \mu_q^2 Q_0 + [\beta - \mu_p + \mu_q][r_{i1} Q_0 - r_{o1} P_0]}{(\beta - \mu_p)P_0 - \mu_q Q_0} \right\}, \tag{22}$$

where  $r_{i1} = r_i(N(0)) = r_i(1), r_{o1} = r_o(N(0)) = r_o(1)$ . From the last two equations we get

$$\frac{k_+}{k_-} = \left\{ \frac{[(\beta - \mu_p)P_0 - \mu_q Q_0]^2}{[(\beta - \mu_p)P_0 - \mu_q Q_0]^2 - \{(\beta - \mu_p)^2 P_0 + \mu_q^2 Q_0 + [\beta - \mu_p + \mu_q][r_{i1} Q_0 - r_{o1} P_0]\}} \right\}. \quad (23)$$

As an example, the case:  $\mu_q = Q_0 = 0$  and  $P_0 = 1$ , considered in [16] reduces the above to  $k_+ = \beta - \mu_p$ ,  $k_- = r_{o1}$  and  $k_+/k_- = (\beta - \mu_p)/r_{o1}$ . While Gyllenberg and Webb chose specific forms for  $r_o$  and  $r_i$  to get  $k_+ = k_- = 1$  for  $\beta - \mu_p = 1$ , our analysis shows that any  $r_o$  and  $r_i$  satisfying (16), where  $r_{o1} = 1$  will be sufficient for this solution.

### 5.2. Solutions for the proliferating and quiescent subpopulations

By using the characteristic relationship (15) we show (see Appendix A), that Eqs. (11) and (12) are equivalent. Assuming (13) we can then solve Eq. (12) for  $P$ ,

$$P = \frac{\mu_q + k_+ e^{-k_- t}}{\beta - \mu_p + \mu_q} N = P_0 \frac{\mu_q + k_+ e^{-k_- t}}{\mu_q + k_+} N, \quad (24)$$

where

$$N(t) = \exp\left\{ \frac{k_+}{k_-} [1 - e^{-k_- t}] \right\}. \quad (25)$$

The solution for quiescent subpopulation is given by

$$Q = N - P = \frac{\beta - \mu_p - k_+ e^{-k_- t}}{\beta - \mu_p + \mu_q} N = \frac{\mu_q Q_0 + k_+ [1 - e^{-k_- t} (1 - Q_0)]}{\mu_q + k_+} N. \quad (26)$$

For  $t \rightarrow \infty$

$$P_\infty = \frac{\mu_q P_0 N_\infty}{\mu_q + k_+}, \quad Q_\infty = \frac{\mu_q Q_0 + k_+}{\mu_q + k_+} N_\infty. \quad (27)$$

Clearly, the normalized final size of proliferating subpopulation,  $P_\infty/P_0$ , is smaller for faster growing tumors (larger  $k_+$ ) with the same death rate  $\mu_q$  and the carrying capacity  $N_\infty$ .

Eq. (24) reveals that the growth fraction,  $P_{\text{frac}} = \frac{P}{N}$ , a measurable quantity which characterizes the growth, is a simple linear combination of a constant and of retardation exponential function:

$$P_{\text{frac}} = \frac{\mu_q + k_+ e^{-k_- t}}{\mu_q + k_+} P_0. \quad (28)$$

It is clear from Eq. (28) that  $P_{\text{frac}}$  is a continuously decreasing function of time irrespectively of whether  $r_i(N)$  and  $r_o(N)$  are monotone functions or not. This is at variance with the statement in the paper of Gyllenberg and Webb which required  $r_i(N)$  to be non-increasing and  $r_o(N)$  non-decreasing [16, p. 27].

In the following we will explore the behavior of  $P(t)$ . Solving Eq. (12) for  $P(t)$  and differentiating,

$$\dot{P}(t) = \frac{\ddot{N} + \mu_q \dot{N}}{\beta - \mu_p + \mu_q} = \frac{\dot{N}(\delta - k_- + \mu_q)}{\beta - \mu_p + \mu_q}. \quad (29)$$

Since for growth  $\dot{N}(t) > 0$  for all finite times, the sign of  $\dot{P}(t)$  is determined by the term  $\delta - k_- - \mu_q = k_+ \exp(-k_- t) - k_- + \mu_q$ . If  $\mu_q > k_- - k_+$ , then  $\dot{P}(0) > 0$  and the proliferating subpopulation will grow initially from time  $t = 0$ . Tumor growth is implied when  $k_+ > k_-$  and the inequality  $\mu_q > k_- - k_+$  is satisfied trivially. If  $\mu_q \geq k_-$ , then  $\dot{P}(t) > 0$  for all finite times and  $P(t)$  will increase monotonically to  $P(\infty) = P_\infty$ . However, if  $\mu_q < k_-$ , then  $P(t)$  will reach a peak level before decreasing to  $P_\infty$ . By solving equation  $k_+ \exp(-k_- t) - k_- + \mu_q = 0$  one finds that the maximum is obtained at time

$$t_{\max} = \frac{1}{k_-} \ln \frac{k_+}{k_- - \mu_q}. \quad (30)$$

Interestingly, the peak in  $P(t)$  is obtained after the time  $t_i$  when the inflection in  $N(t)$  occurs; from (4) and (30) it follows

$$t_{\max} = t_i + \frac{|\ln(1 - \mu_q/k_-)|}{k_-}. \quad (31)$$

The peak in  $P(t)$  is given by (cf. Eq. (3))

$$P_{\max} = P_0 \frac{k_-}{\mu_q + k_+} \exp\left(\frac{k_+ + \mu_q - k_-}{k_-}\right) = \frac{P_0 N_\infty^{1+\mu_q/k_+}}{(1 + \mu_q/k_+)e \ln N_\infty}. \quad (32)$$

The normalized peak,  $P_{\max}/P_0$ , considered as a function of  $k_+ > 0$  is monotonically decreasing (as seen by the analysis of the corresponding derivative), i.e. it becomes smaller for faster growing tumors with the same  $\mu_q$  and  $N_\infty$ , in parallel to the behavior of  $P_\infty/P_0$  noted earlier. Eq. (32) also shows that because of  $\mu_q < k_-$ , the peak value is subject to the following upper bound:

$$\frac{P_{\max}}{P_0} < \frac{k_-}{k_+} \exp\left(\frac{k_+}{k_-}\right) = \frac{N_\infty}{\ln N_\infty}. \quad (33)$$

From (27) one can similarly obtain the upper bound for  $P_\infty$

$$\frac{P_\infty}{P_0} < \frac{N_\infty}{1 + \ln N_\infty}, \quad (34)$$

when  $\mu_q \geq k_-$  the same right-hand side of (34) becomes the lower bound

$$\frac{P_\infty}{P_0} \geq \frac{N_\infty}{1 + \ln N_\infty}. \quad (35)$$

Quiescent subpopulation does not exhibit maximum, but rather monotonically increases towards its limiting value. Indeed, Eqs. (29), (9) and (17) imply

$$\dot{Q} = \frac{\dot{N}(\beta - \mu_p + k_- - \delta)}{\beta - \mu_p + \mu_q} > 0 \quad (36)$$

for all finite times.

### 5.3. Net transition rate

We defined the net transition rate as the difference between the rate at which the cells leave the proliferating subpopulation (out-rate) and the rate at which the cells enter the proliferating subpopulation (in-rate) (see Fig. 2):

$$\Phi(N) = r_o P - r_i Q. \tag{37}$$

Using Eqs. (9), (12) and (13), we can derive

$$\delta = (\beta - \mu_p) \frac{P}{N} - \mu_q \frac{Q}{N} \tag{38}$$

and substitute this into Eq. (14) to find

$$\Phi(N) = k_- \left\{ \frac{(\beta - \mu_p)P - \mu_q Q}{\beta - \mu_p + \mu_q} \right\} + (\beta - \mu_p + \mu_q) \left\{ \frac{PQ}{N} \right\}. \tag{39}$$

The right-hand side of Eq. (39) is greater or equal to zero, because  $(\beta - \mu_p)P - \mu_q Q = \dot{N} \geq 0$  and  $\mu_q \geq 0, \beta - \mu_p \geq 0$ . The net transition is such that it always depletes the proliferating subpopulation, except possibly at  $t = \infty$  if  $\mu_q = 0$  since (see Eq. (14))

$$\Phi(N_\infty) = \left[ \frac{\mu_q(\beta - \mu_p)}{\beta - \mu_p + \mu_q} \right] N_\infty. \tag{40}$$

In Appendix B, we show that  $\Phi(N)$  reaches it maximum value for  $N > N_i$ .

## 6. Simulations and discussion

To illustrate the analytical results obtained, here we show some simulations using the values for  $k_+$  and  $k_-$  determined by fitting tumor growth data to Gompertz function. We used data from Table 4 in [8] which summarizes the values of these parameters for parathyroid tumors as well as for multiple myeloma [3] and testicular tumors [28]. The top panels of Fig. 3 show growth curves for three combinations of  $k_+$  and  $k_-$  as indicated. The first two panels (parathyroid tumors) correspond to the same carrying capacity  $e^{20.6}$  but different maximal growth rates (the rates at inflection points  $\dot{N}(t_i) = N_i(k_+ - k_- \log N_i) = k_- \exp(k_+/k_- - 1)$ ):  $4.36 \times 10^7$  and  $1.02 \times 10^8$  in inverse years. The third (multiple myeloma) differs from the first two both in carrying capacity, ( $e^{28.6}$ ) and in maximal growth rate ( $4.15 \times 10^{12} \text{ yr}^{-1}$ ).

The middle panels of Fig. 3, corresponding to the top growth curves, illustrate proliferation subpopulation profiles for various death rate parameters  $\mu_q$ . As  $\mu_q$  increases, so does the proliferating subpopulation reflecting the requirement that the total cell population growth is maintained. The first set of profiles illustrates that for  $\mu_q = 0.2 > k_-$  (in  $\text{yr}^{-1}$ ) there is no maximum as we concluded in Section 5.2. It should be noted that varying  $\mu_q$ , while  $k_+/k_-$  is constant, must result in changes of  $\beta - \mu_q, r_{i1}, r_{o1}$  according to (23). When comparing the first two set of profiles for  $P(t)$  (which correspond to the same carrying capacity) we observe that slower growing tumors have larger proliferating subpopulation at later times in agreement with (27). Consequently, cancer therapy which affects only proliferating cells may not suffice to eradicate these cells in slower growing tumors, but could be sufficient to eradicate proliferating cells in faster growing tumors, which was clinically observed.

The bottom panels of Fig. 3 illustrate monotonically decreasing growth fraction (normalized by initial proliferation subpopulation) for the same set of  $\mu_q$ . The first two cases (Fig. 3(c) and (f)) show that at any given time the growth fraction is larger for the larger death rate of quiescent cells

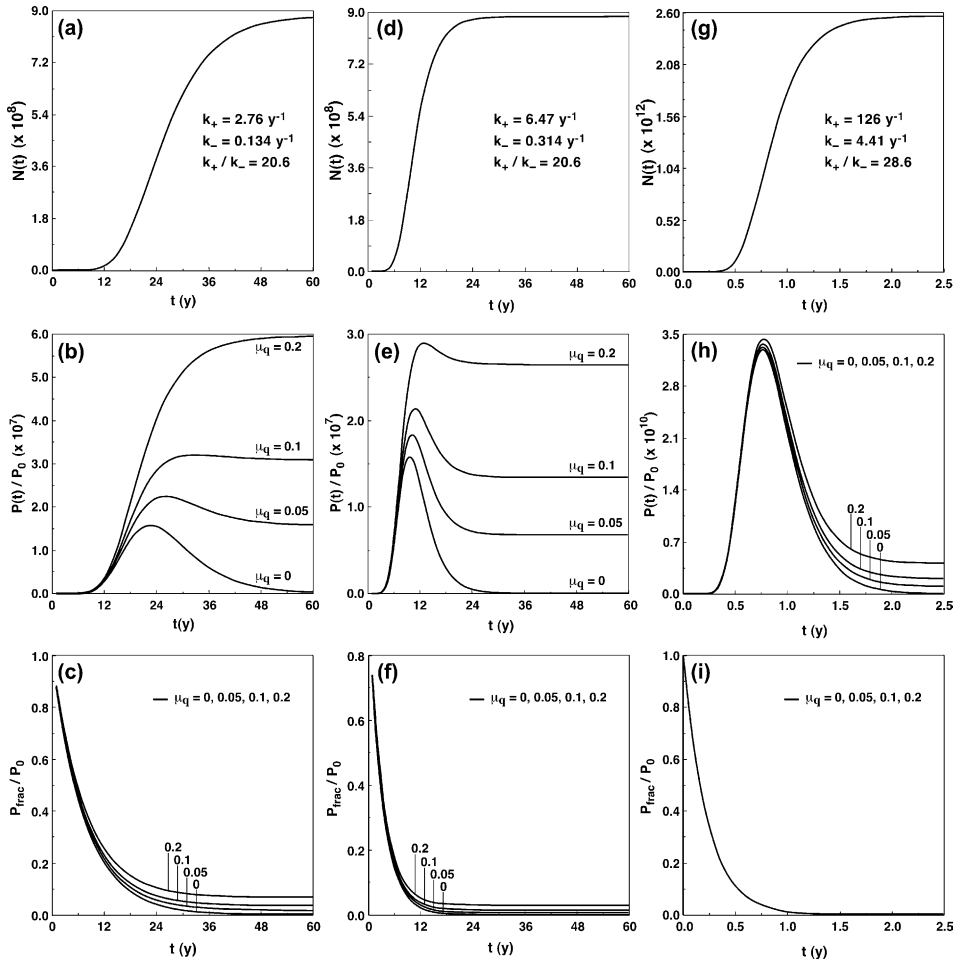


Fig. 3. Comparison of tumor growth curves (panels a, d, g), corresponding proliferating subpopulations (panels b, e, h) and growth fractions (panels c, f, i) for various growth rate constants  $k_+$ , retardation rate constants  $k_-$  and death rates  $\mu_q$ . All rates are given in inverse years. Panels (a) and (d) depict growth curves for parathyroid tumors, and panel (g) corresponds to multiple myeloma. The rate constants are taken from Table 4 in [8] and the values for  $\mu_q$  are chosen to exemplify the influence on  $P(t)$  and  $P_{frac}$ .

in agreement with the notion that increased cell death drives growth. Of course, the expression (28) shows this analytically, since the derivative of  $P_{frac}$  as a function of  $\mu_q$  is non-negative. In the third case (Fig. 3(i)) there seems to be no effect of changing  $\mu_q$  at the given scale, which is the consequence of relatively small values of  $\mu_q$  compared to the values of  $k_+$  and  $k_-$ .

Gyllenberg and Webb conservatively assumed that  $r_o(N)$  was non-decreasing and  $r_i(N)$  non-increasing. The present model requires only that  $r_o(N) \geq 0$  and  $r_i(N) \geq 0$  obey Eq. (15), or equivalently, that for any  $r_i(N) \geq 0$ , the corresponding  $r_o(N)$  is given by (16) assuming necessary condition  $\beta - \mu_p \geq k_+$ . We will construct  $r_i(N)$  which increases during the early part of the Gompertz growth reaching the maximum and then decreases. In the following we analyze the effect of different values of  $\mu_q$ , on transition rate function  $r_o(N)$ , on complete transition rates

$r_i(N)Q$ ,  $r_o(N)P$  and on net transition rate function  $\Phi(t)$ . In case  $\mu_q = 0$  it follows that  $r_{i\infty} = r_i(N_\infty) = 0$ , i.e. the constructed  $r_i$  must be zero at  $t = \infty$ . We use

$$r_i(N) = 0.25[1 + 2 \ln N]\delta(N). \tag{41}$$

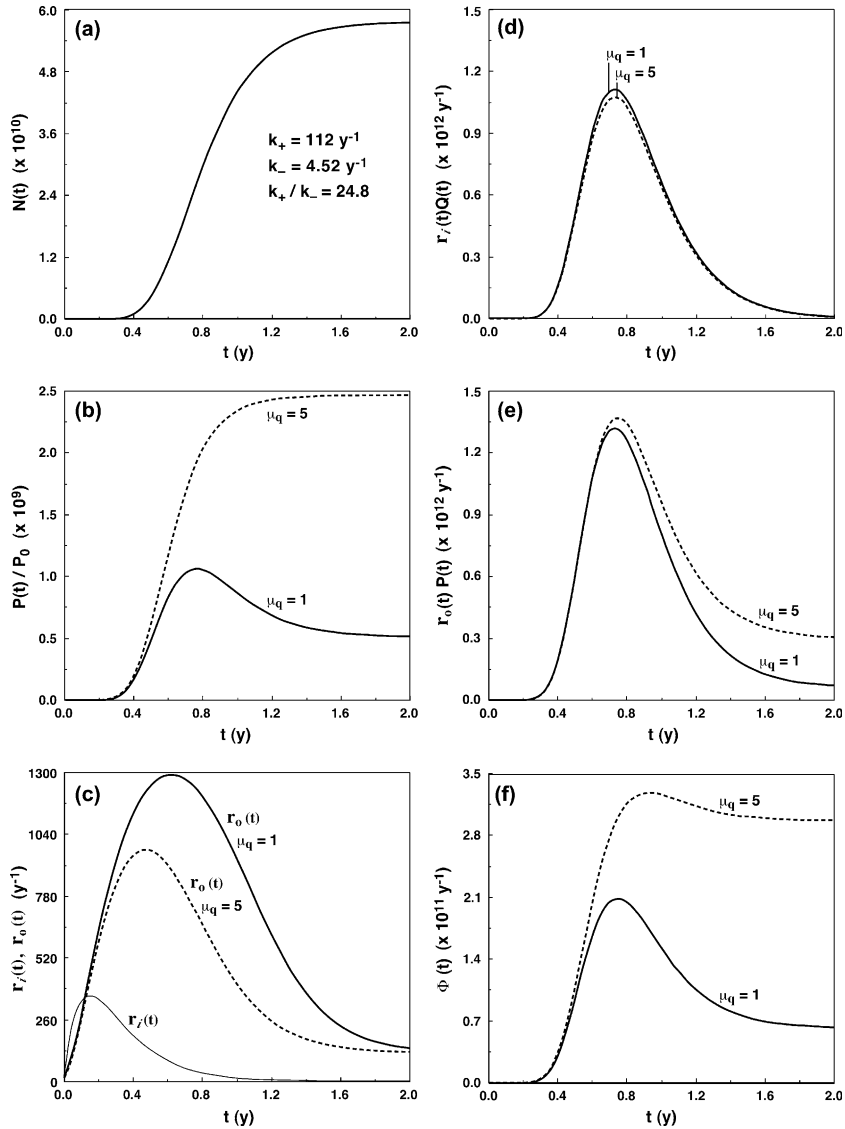


Fig. 4. Dependence of transition rates on quiescent cell death rate. Panel (a) shows a Gompertzian growth of a testicular tumor ( $k_+$  and  $k_-$  from Table 4 of [8]). Panel (b) shows the corresponding proliferating subpopulation for two values of quiescent cell death rate. Panel (c) shows related transition rate functions between proliferating and quiescent cell compartments, while in panels (d) and (e) the corresponding complete transition rates are depicted (see text). Panel (f) shows that the net transition rate from  $P$  to  $Q$  is always positive and remains different from zero even for infinite times (see Eq. (40)).

(Note:  $\delta(N_\infty) = 0$ .) For  $k_+$  and  $k_-$  we have chosen values for testicular tumors provided in Table 4 of [8] and in addition we assumed  $\beta - \mu_p = 120 \text{ yr}^{-1}$  being greater than  $k_+ = 112 \text{ yr}^{-1}$  as required by (17). We also assumed that initially the whole cell population is proliferating ( $P_0 = 1, Q_0 = 0$ ). The simulations are presented in Fig. 4. Again as  $\mu_q$  increases,  $P$  increases and  $r_o$  decreases in value, reflecting the system's need to maintain higher productivity to make up for the increasing loss, while holding the total number of cells constant at the comparable time. The transition out-rate of the proliferating compartment,  $r_o P$ , increases with increasing  $\mu_q$  to make up for the losses from the quiescent subpopulation. The transition in-rate,  $r_i Q$ , decreases only slightly reflecting the decrease in  $Q$  for an increasing  $P$ , since  $r_i$  is unchanged by change of  $\mu_q$ . The net transition rate (Fig. 4(f)) shows maximum as analytically predicted, even when the proliferating subpopulation does not reach its maximum in final times (Fig. 4(b),  $\mu_q = 5$ ).

The above illustrations exemplify some interesting kinetic features of cell proliferation, when the Gompertz and Gyllenberg–Webb model are combined. While these features have to be further investigated in the context of experimental and clinical data, the analytical results obtained provide relatively simple mathematical basis for quantitative analysis of tumor growth. In particular, one can fit tumor growth data for total cell population and obtain parameters  $k_+$  and  $k_-$ . Subsequently one can fit the simple expression (24) for  $P(t)$  to data for proliferating subpopulation. This would yield values for  $\mu_q$  and  $\beta - \mu_p$ . (Note that  $\beta$  and  $\mu_p$  cannot be determined separately by fitting, as already Eqs. (7) and (8) imply.) Once the values of these parameters are established, one can use the model to simulate tumor growth in response to proposed therapy, which could change either proliferation rate constant  $\beta$  or induce cell death, thus changing  $\mu_q$  and/or  $\mu_p$ .

In the described procedure the model parameters are determined without need to first specify rate functions  $r_o(t)$  and  $r_i(t)$ , and then, in the process of fitting, numerically solve the system of differential Eqs. (7) and (8). This would be the standard approach in application of the original Gyllenberg–Webb model to tumor growth data. By assuming that the Gompertz model is a good deterministic descriptor of total tumor cell population growth (which has been reasonably well verified), we have shown how to obtain information about proliferating and quiescent cell populations without the problem of specifying transition rate functions.

## 7. Conclusion

The hybridization of Gompertz and Gyllenberg–Webb models presented is based on the assumption that the latter should predict Gompertz growth when the net inter-compartmental transition rate function satisfies relationship Eq. (14). This is a sufficiently general relation to make the hybrid model robust in the allowable forms of the transition rate functions. Furthermore, this hybrid model provides expressions for Gompertz growth and retardation parameters,  $k_+$  and  $k_-$  in terms of the cell kinetic parameters defined by Gyllenberg–Webb model. The general solutions for proliferating and quiescent subpopulations are given in an analytic form, and by simulations we demonstrated the importance of the quiescent cell death rate as one of determining factors of the size of these subpopulations. Relationships among  $k_+$ ,  $k_-$  and  $\mu_q$  determine whether the proliferating subpopulation grows past its initial level and it also determines the final equilibrium value. The net inter-compartment transition rate is predicted to always be from

proliferating compartment to the quiescent compartment. All of these characteristics can be of interest in modeling response of tumors to therapeutic insult or stimulation of T lymphocytes.

In the final note, we wish to point out that the method implemented here for obtaining the size of proliferating and quiescent subpopulation, based on postulated total cell population kinetics, can be modified to incorporate other than the Gompertz model. For example one can assume that the Bertalanffy–Richards (or modified Verhulst) model best describes growth curves, as suggested in [29] where primary breast cancer data were analyzed. Then one can combine the Gyllenberg–Webb model with the Bertalanffy–Richards model for the total cell population, and obtain similar analytical results for proliferating and quiescent subpopulations.

### Acknowledgements

We thank Mr Ken Peters for his valuable assistance in preparation of figures. This work is supported in part by Mayo Clinic Cancer Center.

### Appendix A

We show the equivalence of Eqs. (11) and (12) when the relationship (14) is assumed. To simplify the notation, we introduce the following:  $m := \beta - \mu_p + \mu_q$ . Then Eqs. (11), (12) and (15) become

$$\dot{P} = (\beta - \mu_p)P - \Phi(N), \tag{A.1}$$

$$\dot{N} = mP - \mu_q N, \tag{A.2}$$

$$\Phi(N) = N \left[ \frac{\{k_- - \mu_q - \delta(N)\}\delta(N)}{m} \right] + N \left[ \frac{(\beta - \mu_p)(\delta(N) + \mu_q)}{m} \right]. \tag{A.3}$$

Starting with Eq. (A.2) and using Eq. (13), we have

$$P = \frac{\dot{N} + \mu_q N}{m} = \frac{(\delta + \mu_q)N}{m}, \quad \dot{P} = \frac{N\{\delta(\delta + \mu_q - k_-)\}}{m}. \tag{A.4}$$

We can now substitute  $\delta(\delta + \mu_q - k_-)$ , appearing in the expression for  $\dot{P}$ , from the right-hand side of Eq. (A.3). Then by the use of Eq. (A.4) for  $P$ , we obtain

$$\dot{P} = \frac{(\beta - \mu_p)(N\mu_q + N\delta)}{m} - \Phi(N) = (\beta - \mu_p)P - \Phi(N). \tag{A.5}$$

This is Eq. (A.1). Now starting with Eq. (A.1) and substituting for  $\Phi(N)$  from Eq. (A.3) we have

$$\dot{P} = (\beta - \mu_p)P - N \left[ \frac{\{k_- - \mu_q - \delta(N)\}\delta(N)}{m} \right] - N \left[ \frac{(\beta - \mu_p)(\delta(N) + \mu_q)}{m} \right]. \tag{A.6}$$

Defining  $X := \frac{N(\mu_q + \delta)}{m}$  with  $\dot{X} = \frac{N\delta(\mu_q + \delta - k_-)}{m}$  and  $Y := (P - X)$ , Eq. (A.6) can be written  $\dot{Y} = (\beta - \mu_p)Y$ . The solution to this equation is in the form

$$Y = Y_0 \exp\{(\beta - \mu_p)t\}. \quad (\text{A.7})$$

But  $Y_0$  can be shown to be zero using  $P_0 + Q_0 = 1$  and Eq. (18). Then  $P = X$  and upon using (13), one obtains (A.2).

## Appendix B

We show that  $\Phi(N)$  reaches a maximum value after the inflection point of  $N$ , i.e. for  $N > N_i$ . Differentiating Eq. (14) with respect to time and using Eq. (13) we obtain

$$\dot{\Phi}(N) = \frac{\dot{N}}{m} \left[ -(\delta - k_-)^2 + (\beta - \mu_p - \mu_q + k_-)(\delta - k_-) + \mu_q(\beta - \mu_p) + k_-^2 \right]. \quad (\text{B.1})$$

Since  $\dot{N}$  is always positive,  $\dot{\Phi}(N)$  gets its sign from the term in the brackets. The bracketed term is a concave down quadratic in  $x = \delta - k_-$  with its vertex in the first quadrant. From Eq. (13) we get that  $k_- = \delta(N_i)$ . The ‘y’ intercept of the quadratic occurs at the inflection point of  $N$  and since  $\delta$  is a decreasing function of  $N$ , the  $x$  intercept ( $\dot{\Phi}(N) = 0$ ) occurs after  $N$  has reached inflection.

## References

- [1] A.K. Laird, Dynamics of tumor growth, *Br. J. Cancer* 18 (1964) 490.
- [2] L. Simpson-Herren, H.H. Lloyd, Kinetic parameters and growth curves for experimental tumor systems, *Cancer Chemother. Rep.* 54 (1970) 143.
- [3] P.W. Sullivan, S.E. Salmon, Kinetics of tumor growth and regression in igG multiple myeloma, *J. Clin. Invest.* 51 (1972) 1697.
- [4] L. Norton, A Gompertzian model of human breast cancer growth, *Cancer Res.* 48 (1988) 7067.
- [5] R. Demicheli, R. Forni, A. Ingrosso, G. Pratesi, C. Soranzo, M. Tortoreto, An exponential-Gompertzian description of LoVo cell tumor growth in vivo and in vitro data, *Cancer Res.* 49 (1989) 6543.
- [6] M. Marušić, Ž. Bajzer, J.P. Freyer, S. Vuk-Pavlović, Tumor growth in vivo and as multicellular spheroids compared by mathematical models, *Bull. Math. Biol.* 56 (1994) 617.
- [7] I.D. Bassukas, Comparative Gompertzian analysis of alterations of tumor growth, *Cancer Res.* 54 (1994) 4385.
- [8] A.M. Parfitt, D.P. Fyhrie, Gompertzian growth curves in parathyroid tumors: further evidence for the set-point hypothesis, *Cell Proliferat.* 30 (1997) 341.
- [9] Ž. Bajzer, S. Vuk-Pavlović, Mathematical modeling of tumor growth kinetics, in: J. Adam, N. Bellomo (Eds.), *A Survey of Models for Tumor-Immune System Dynamics*, Birkenhauser, Boston, MA, 1997, p. 89.
- [10] R. Chignola, A. Schenetti, G. Andrighetto, E. Chiesa, R. Foroni, S. Sartoris, G. Tridente, D. Liberati, Forecasting the growth of multicell tumor spheroids: implications for the dynamic growth of solid tumors, *Cell Proliferat.* 33 (2000) 219.
- [11] W.R. Miller, D.A. Cameron, A.A. Ritchie, The relative importance of proliferation and cell death in breast cancer growth and response to tamoxifen, *Eur. J. Cancer* 37 (2001) 1533.
- [12] M.A. Savageau, Allometric morphogenesis of complex systems: a derivation of the basic equations from first principles, *Proc. Nat. Acad. Sci. USA* 76 (1979) 6023.
- [13] M. Witten, A return to time, cells, systems, and aging: III. Gompertzian models of biological aging and some possible roles for critical elements, *Mechanisms Aging Dev.* 32 (1985) 141.
- [14] W.S. Kendal, Gompertzian growth as a consequence of tumor heterogeneity, *Math. Biosci.* 73 (1985) 103.

- [15] C.L. Frenzen, J.D. Murray, A cell kinetics justification for Gompertz' equation, *SIAM J. Appl. Math.* 46 (1986) 614.
- [16] M. Gyllenberg, G.F. Webb, Quiescence as an explanation of Gompertzian tumor growth, *Growth, Dev. Aging* 53 (1989) 25.
- [17] C.P. Calderón, T.A. Kwembe, Modeling tumor growth, *Math. Biosci.* 103 (1991) 97.
- [18] R. Makany, A theoretical basis for Gompertz's curve, *Biometr. J.* 33 (1991) 121.
- [19] Y. Ling, B. He, Entropic analysis of biological growth models, *IEEE Trans. Biomed. Eng.* 40 (1993) 1193.
- [20] A.-S. Qi, X. Zheng, C.-Y. Du, B.-S. An, A cellular automaton model of cancerous growth, *J. Theor. Biol.* 161 (1993) 1.
- [21] Ž. Bajzer, Gompertzian growth as a self-similar and allometric process, *Growth, Dev. Aging* 63 (1999) 3.
- [22] E.K. Afenya, C.P. Calderon, Diverse ideas on the growth kinetics of disseminated cancer cells, *Bull. Math. Biol.* 62 (2000) 427.
- [23] Ž. Bajzer, S. Vuk-Pavlović, New dimensions of Gompertzian growth, *J. Theor. Med.* 2 (2000) 307.
- [24] J.C.M. Mombach, N. Lemke, B.E. Bodmann, M.A.P. Idiart, A mean-field theory of cellular growth, *Europhys. Lett.* 59 (2002) 923.
- [25] F.G. Sherman, H. Quastler, Cell population kinetics in the intestinal epithelium of the mouse, *Exp. Cell Res.* 17 (1959) 420.
- [26] J. Schiller, M. Eisen, Stability analysis of normal and abnormal neoplastic growth, *Bull. Math. Biol.* 39 (1977) 597.
- [27] S. Piantadosi, A model of growth with first-order birth and death rates, *Comput. Biomed. Res.* 18 (1985) 220.
- [28] R. Demicheli, Growth of testicular lung metastasis: tumor specific relation between two Gompertzian parameters, *Eur. J. Cancer* 16 (1980) 1603.
- [29] J.A. Spratt, D. von Fournier, J.S. Spratt, E.E. Weber, Decelerating growth and human breast cancer, *Cancer* 71 (1993) 2013.